# Direct estimation of capture cross sections in the presence of slow capture: application to the identification of quenched-in deep-level defects in Ge

S. H. Segers,[1] J. Lauwaert,[1] P. Clauws,[1] E. Simoen,[1,2] J. Vanhellemont,[1] F. Callens,[1] and H. Vrielinck[1,*]

[1] *Department of Solid State Sciences, Ghent University, Krijgslaan 281-S1, 9000 Gent, Belgium*
[2] *IMEC, Kapeldreef 75, 3010 Leuven, Belgium*

Quenching experiments have been performed on both n- and p-type Ge in a dedicated furnace using infrared lamp heating. The capture and emission characteristics of the induced deep-level defects in the quenched samples were investigated by means of Deep Level Transient Spectroscopy. For all defect levels, a high impact of capture in the transition region (slow capture) was found. An empirical approach to analyse this effect is presented, which allows to extract reliable capture cross-section parameters. The defect parameters thus obtained were compared with previously published data and it was found that some prominent quenching-induced deep levels are related to metal impurities (Cu and Ni), while others may be vacancy-related.

PACS numbers: 71.55.Cn, 72.20.Jv

## I. INTRODUCTION

Germanium is an important material in advanced electronic devices such as optical detectors, high-efficiency solar cells and radiation detectors, due to its high carrier drift mobility, low band gap and high atomic number.[1] For the processing of these devices, rapid thermal annealing is often applied. Single crystal growth obviously also occurs at high temperatures. Therefore, one may expect considerable concentrations of intrinsic defects, which, upon cooling, can interact with dopants and/or contaminants and can give rise to deep levels in the band gap of the material. These deep levels can have a significant effect on the electric properties of the material (e.g. carrier lifetime). Nevertheless the thermodynamic properties of intrinsic defects in Ge are still largely unexplored. A well-known method for obtaining such information is rapid thermal quenching.[2–5]

Previous experiments generally established that quenching introduces acceptor-like defects in Ge.[2–10] These have been attributed to vacancy related defects[2, 6, 11–13], but also transition metal (TM) contamination has been suggested to play an important role in the formation of quenched-in acceptors.[6, 10, 11, 14–16] In particular, Cu is known to have a high solubility and diffusivity in germanium at elevated temperatures ($> 500°$C), as has e.g. been monitored by spreading resistance measurements on Cu-diffused Ge samples.[7, 17, 18] The properties of Cu-related point defects in Ge, their interaction with other point defects, precipitation and gathering have been reviewed by Bracht.[19]

Deep-Level Transient Spectroscopy (DLTS)[20] is one of the most powerful techniques to study deep levels due to its high sensitivity and resolution. The interpretation in terms of defect models is, however, often not unambiguous and in particular in the context of quenched-in defects in Ge, the nature of deep-level defects is still controversial.[6, 10] In the past decade, the knowledge of TM-related deep levels in Ge has further increased[21–25], and perhaps even more relevant in this context, comprehensive DLTS studies on electron and heavy-particle irradiated Ge have yielded information on the stability and electronic levels of vacancy- and interstitial Ge-related defects in Ge.[26–35] With this in mind, we performed a new DLTS study on quenched p-type (Section III A) and n-type Ge (Section III B), using an infrared (IR)-lamp based oven for heating. The cooling rate obtained by this quenching-set up is significantly larger than that obtained in rapid thermal annealing/processing (RTA/RTP) experiments, which was shown to be too low for inducing intrinsic defects. [6, 36] For all deep defect levels observed in quenched Ge samples, next to the defect signatures, determined in Section III A 1 (apparent activation enthalpy $\Delta E_A$ and pre-exponential factor $K_T$), the capture cross-section $\sigma_p$ of the defect levels has been determined separately via pulse width variation experiments. The analysis of these experiments was found to be complicated by capture in the transition region at the edge of the depletion layer, which we will further label here as "slow capture".[37, 38] $\sigma_p$ proved to be a very important parameter for the identification of quenched-in defects in Ge via comparison with literature results in Section IV. For this reason, in Section III A 2, we propose an empirical approach to estimate this parameter, taking into account the effect of slow capture.

## II. EXPERIMENTAL DETAILS

The starting materials were p-type Ge samples cut from 8 inch diameter wafers with a Ga shallow acceptor concentration of $6\times10^{14}$ cm$^{-3}$ and from n-type Ge wafers with an Sb shallow donor concentration of $2\times10^{14}$ cm$^{-3}$, both supplied by Umicore Electro-Optic Materials. The samples were cleaned in a $HNO_3$:HF (3:1) solution before

*Electronic address: henk.vrielinck@ugent.be

the thermal treatment.

The heating itself occurred in a dedicatedly designed IR-lamp based oven, schematically shown in figure 1. This oven consists of a T-shape quartz tube, surrounded by four 2 kW tungsten halogen lamps with quartz reflective coating. Two highly doped (p-type, $10^{19}$ cm$^{-3}$ B) Si plates are mounted horizontally in the tube, spaced by two quartz rods (4 cm spacing). These Si plates absorb the IR light and provide indirect heating, like in an RTA/RTP setup. The sample is placed on the bottom Si plate, close to an opening in this plate, above the vertical component of the quartz tube. Between the two Si plates, a quartz push rod, on the one side, and two thermocouples, protected by quartz tubes, on the other side, are placed. For heating, the sample is positioned about 2 cm in front of the opening. Between room temperature (RT) and 900°C, the heating is performed at a rate of 6°C/s, with a maximum overshoot of 2°C. To prevent oxidation, the quartz tube is continuously flushed with Ar during the heating process. At a time $t_Q$ (heating time) after stabilization of the oven at heating temperature $T_H$, a valve on the bottom of the quartz tube, closing off the tube during heating, is opened, the sample is pushed through the opening in the bottom silicon plate, and falls into a recipient with the quenching medium. Because quenching in water resulted in shattered samples, silicone oil was chosen as a quenching medium. Although this medium provides a lower cooling rate than water, the cooling rate is still considerably higher than when using a gas as cooling medium (like in RTA experiments).

The time between opening the valve and the sample falling into the quenching medium is $\sim 1.5$ s. After the quench and a short etch, some samples were given a post-anneal at 300°C during 60 min., and slowly cooled in the oven.

The p-type (n-type) samples were prepared for DLTS measurements by evaporating In (Au) to form a Schottky junction. This evaporation was preceded by a short etch in a $HNO_3$:HF (3:1) solution to clean the sample surface and to remove all native oxide. Ohmic contacts were prepared using In-Ga eutectic and In foil. Capacitance DLTS measurements were performed with a Fourier transform instrument (Phystech FT1030) equipped with a Boonton 72B capacitance meter with an AC test signal of 1 MHz. The sample was placed in a Heraeus contact gas liquid He cryostat, equipped with four heat shields to avoid black-body radiation. During the DLTS measurements, capacitance transients were recorded at reverse voltage $V_R$ <0 after a filling pulse (duration $t_P$) to pulse voltage $V_P$ ($V_R < V_P$ <0) and a waiting time $t_0$, typically $t_W/512$ for temperature sweeps and $t_W/4$ for isothermal measurements ($t_W$: rate window time). In all DLTS spectra in this paper, the $b_1$ Fourier component is shown:

$$b_1 = \frac{2A}{t_W} exp\left(-\frac{t_0}{\tau}\right)\left[1 - exp\left(-\frac{t_W}{\tau}\right)\right]\frac{\omega}{\frac{1}{\tau^2}+\omega^2}, \quad (1)$$

with $A$ the amplitude of the transient, $\tau$ the emission time constant and $\omega = \frac{2\pi}{t_W}$.

## III. EXPERIMENTAL RESULTS

### A. p-type

#### 1. Spectrum & defect signatures

The bulk and surface Cu-concentration of several untreated samples, samples that were only etched, heated and quenched Ge specimens, and samples that were heated for a prolonged time (2h) at elevated temperature (850°C) and slowly cooled was checked with glow discharge mass spectrometry, energy dispersive X-ray spectroscopy, X-ray fluorescence, and X-ray photoelectron spectroscopy. For none of the samples Cu concentrations above the detection limits occurred. In particular, this demonstrates that for none of the Ge samples the bulk Cu concentration (in any form) exceeded 10 parts per billion ($5\times10^{14}$ cm$^{-3}$). The electrically active defects were studied by DLTS. A typical DLTS spectrum of quenched p-type Ge samples is shown in figure 2(a). Five peaks, labeled H1-H5, contribute to this spectrum. No DLTS signals, and in particular no electrically active Cu levels, were observed in measurements before quenching. It is also worth noting that the spectra of samples which were slowly cooled (not quenched), after a similar heat treatment, exhibit clear contributions from H1, H4 and H5, but not of H2 and H3. Arrhenius analysis allowed to determine apparent activation energies $\Delta E_A$ and pre-exponential factors $K_T$ for all peaks observed in this spectrum. These are summarized in Table I. Simulations of individual peaks (figure 2(a)) and of the total spectrum (figure 2(b)) ensure the accuracy of the analysis. The H1, H2 and H4 peaks exhibit a clear Poole-Frenkel (PF) shift. The H3 peak showed no observable field dependence. However, due to its position close to the H4 peak and its smaller amplitude, a slight electric field dependence cannot be excluded. Although the H5 peak is present in all measured spectra, its amplitude seems to vary randomly but always remains much smaller than that of the H4 peak. Between the H1 and H2 peak, an additional, temperature independent emission component is visible for large $t_W$. As previously reported for Ge:Co and Ge:Cr, this emission is related to photoionization as a result of non-complete shielding of the blackbody radiation. [39] This additional emission component has been taken into account for the simulation of the spectrum in figure 2(b).The photoionization effect is only observed when using relatively large rate window times $t_W$, which were necessary here in order to resolve the H3 contribution, appearing as a shoulder on H4.

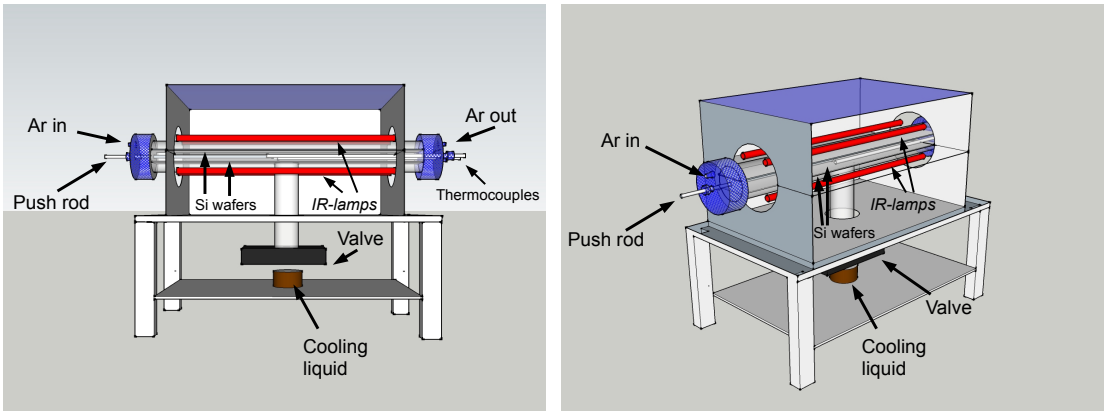


(a)Front view (b)Isometric view

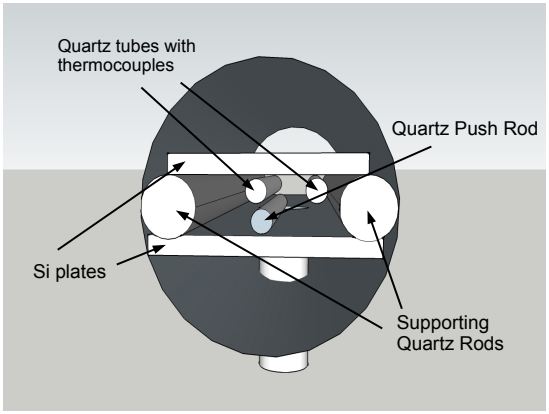


(c)Interior of T-shaped quartz tube

FIG. 1: Quenching set-up

| ID | $\Delta E_A(meV)$ | $K_T(s^{-1}K^{-2})$ | $\sigma_p(cm^2)$ |
|---|---|---|---|
| H1 | 24 | $2.0\times 10^{7}$ | $8.6\times 10^{-13}$ (13K) |
| H2 | 68 | $2.0\times 10^{6}$ | $1.1\times 10^{-13}$ (36K) |
| H3 | 234 | $1.6\times 10^{7}$ | $3.9\times 10^{-14}$ (107K) |
| H4 | 298 | $3.9\times 10^{8}$ | $9.9\times 10^{-14}$ (123K) |
| H5 | 210 | $2.6\times 10^{8}$ | $1.5\times 10^{-13}$ (90K) |
| ID | $\Delta E_A(meV)$ | $K_T(s^{-1}K^{-2})$ | $\sigma_n(cm^2)$ |
| E1 | 356 | $4.3\times 10^{7}$ | $4.8\times 10^{-19}$ (160K) |

TABLE I: Apparent activation energy, pre-exponential factor and capture cross section of the most prominent DLTS peaks in quenched Ge.

### 2. *Capture cross sections*

In order to obtain extra parameters for defect identification, for all hole trap centers observed in the DLTS spectra the capture cross section was also measured independently in pulse length variation experiments. If capture in the transition region can be neglected, the DLTS amplitude is expected to grow with increasing $t_P$ as

$$\Delta C(t_P) = \Delta C_\infty \left(1 - exp\left(\frac{-t_P}{\tau_c}\right)\right) \quad (2)$$

where the capture time constant $\tau_c$ is related with the capture cross section $\sigma_p$ (expression for holes in p-type semiconductor):

$$\tau_c = (p.v_{th,p}.\sigma_p)^{-1} \quad (3)$$

p is the carrier concentration (determined from static C-V measurements) and $v_{th,p}$ the thermal hole velocity. Hence, $\sigma_p$ can be determined by linear regression from the relation

$$ln\left(\frac{\Delta C_\infty - \Delta C(t_P)}{\Delta C_\infty}\right) = -p.v_{th,p}.\sigma_p.t_P \quad (4)$$

Figure 3(a) shows the experimental results for the pulse length variation experiments for the H4 peak in quenched Ge for various values of the reverse voltage. The logarithmic expression on the left hand side of Equation (4) as a function of $t_P$ is shown in figures 3(b) (smallest $V_R$) and 3(c) (all $V_R$). For all $V_R$ values there is a

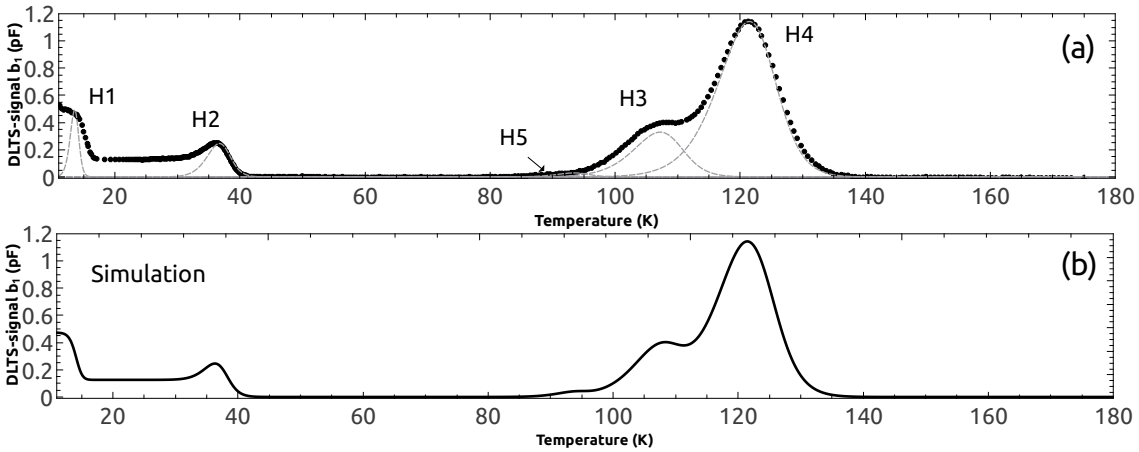


FIG. 2: (a) DLTS spectrum of samples quenched in silicone oil ($t_Q$=60 min, $T_H$=650°C; $V_R$=-1V, $V_P$=-0.2V, $t_W$=512 ms) with peaks simulated using the $\Delta E_A$ and $K_T$ values in Table I. (b) Simulated total spectrum, including the additional emission components on H1 and H2 caused by photoionization.

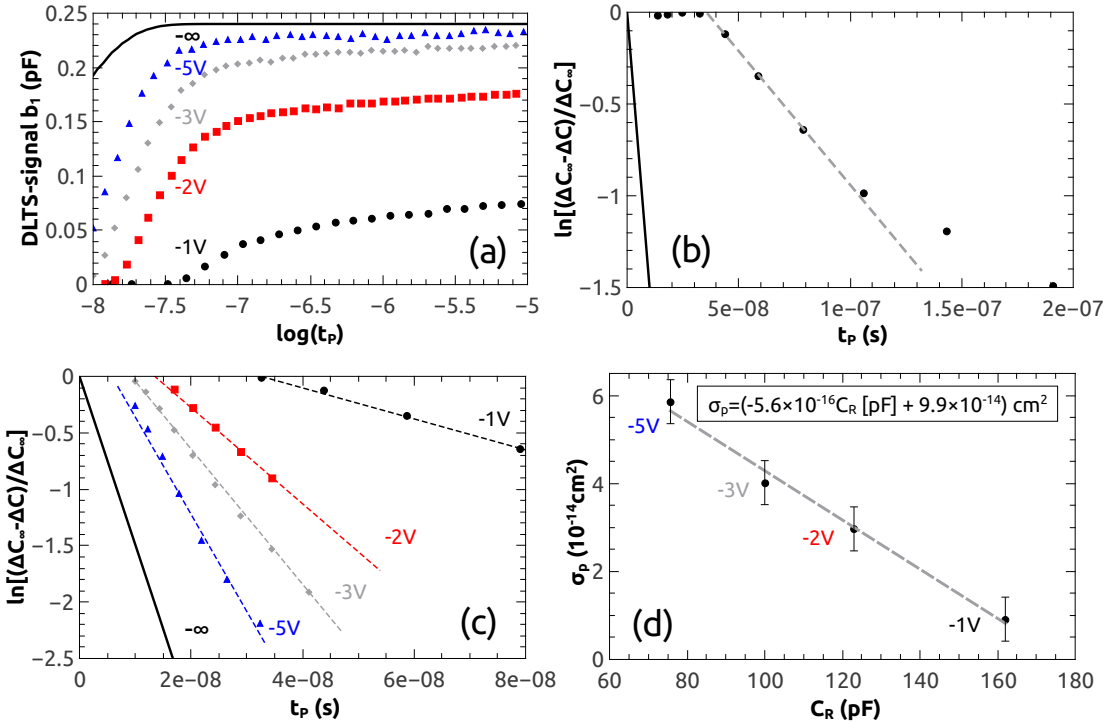


FIG. 3: Analysis precedure of $\sigma_p$ for H4 at T=123K. (a) Pulse width dependence of the DLTS signal for different $V_R$ ($V_P$=-0.2V). (b) Semilogarithmic plot for $V_R$=-1V. The dashed line is used for calculating the apparent value of $\sigma_p$. (c) Semilogaritmic plots for different $V_R$ ($V_P$=-0.2V). Only the points used for estimating $\sigma_p(C_R)$ are plotted. (d) Linear regression on the $\sigma_p(C_R)$ values obtained from (c). The full lines represent relations (2) and (4) for the eventually determined $\sigma_p(C_R$=0) value, in case the influence of slow capture is negligible.

clear deviation from the linear dependence on $t_P$. At large $t_P$ the increment of the DLTS amplitude with $t_P$ is slower than exponential, a well-known effect of capture in the transition region at the edge of the depletion layer (slow capture), that has been studied by Pons et al.[37] and modeled in detail by Lauwaert et al.[38] At small $t_P$, however, the DLTS amplitude growth is also smaller than exponential. This effect has also been attributed to slow capture by Pons et al.[37], but it has -to the best of our knowledge- so far not been explained

how this effect can be dealt with in the capture cross section analysis. In between these two $t_P$ regions, the curves in figures 3(b) and 3(c) appear to exhibit a linear part, which, unlike equation (4), does not pass through the origin. The slope of the linear region increases with applied $|V_R|$ (or depletion width and hence decreasing $C_R$, see figures 3(c)), while the intercept on the $t_P$ axis at zero ordinate ($\Delta C=0$) moves closer to 0. Both facts suggest that at infinitely large $|V_R|$ ($C_R = 0$), equation (4) should hold exactly and should allow to determine the correct value of the capture cross section. Indeed, for an infinitely wide depletion layer, the relative effect of a finite width transition region is expected to vanish. Hence, for obtaining good estimates of the capture cross section, large reverse voltages should be applied to the junction. From an experimental viewpoint $|V_R|$ values are, however, limited by the maximum leakage current the setup can bear and eventually also by breakdown of the diode. Hence, we propose here a practical-empirical solution to the problem of determining $\sigma_p$ in the case of strong effects of slow capture.

From the slope of the linear parts of the curves in figures 3(b) and 3(c), for each value of $V_R$ (or $C_R$) an effective $\sigma_p(C_R)$ value can be calculated, which appeared to exhibit a linear dependence on $C_R$, for all DLTS peaks analyzed here (see figures 3(d) and 4). Hence, we propose to determine $\sigma_p$ by linear extrapolation to $C_R$=0. The values thus obtained are listed in table I and the limiting case relations for negligible effect of slow capture for H4 are plotted in figures 3(a)-3(c) as solid lines. As a check for the consistency of the method, $\sigma_p$(H2) was determined from the thermionic emission component (at T=35K) and from the photoionization component (T=20K) and in both measurements, within experimental accuracy, the same value was determined. Finally, it should be noted that the analysis outlined here shows that slow capture does not necessarily prevent accurate estimation of capture cross sections, but may, on the contrary, facilitate the analysis. Indeed, if $\sigma_p$ is very large, without influence of slow capture, $\Delta C(t_P)$ may immediately saturate in the accessible $t_P$ range ($t_P$ >10-20 ns). As seen in the simulations (solid lines) in figures 3(a) and 3(c), H4 is nearly in this case. If slow capture does exhibit a strong influence, the $\Delta C(t_P)$ curves grow slower and measuring them as a function of $V_R$ may still allow reliable determination of $\sigma_p$.

#### *3. Concentration profiles & post-annealing*

Varying $V_R$ with constant $\Delta V=V_P-V_R$ (= 0.5V) at a constant temperature, one can determine a concentration depth profile of the defects giving rise to the observed peaks. This is shown in figure 5. For H5 the measured concentrations were too low to determine reliable profiles. The depth profile of H1 could not be measured accurately because of the high impact of (small) temperature fluctuations at low temperatures, close to the freeze-out of the samples. The concentrations of H3 and H4 have been separated by peak deconvolution. Within the accessible spatial range from the junction, the profiles for H2, H3 and H4 are fairly flat, suggesting that in- or out-diffusion profiles must extend over at least 10μm. The H2 and H3 peaks have, within experimental error, the same profile which might indicate that they correspond to different charge transition levels of the same defect. Kamiura et al. already argued that this is most probably not the case: the lack of PF shift suggests assignment for H3 to a donor, whereas H2 clearly corresponds to an acceptor level, and for one and the same defect a donor level is not expected to lie above an acceptor level.[10] We already mentioned that the absence of PF shift for H3 cannot be firmly established in view of the overlap with H4, which exhibits a strong PF shift. In addition, the study of Fe and Co defect levels in Ge have shown that conclusions on the donor/acceptor character of levels based on their PF shift is not always unambiguous.[25] Nonetheless, so far for none of the multiple acceptor TM-related levels in Ge a smaller PF shift has been observed for a more highly charged defect level. [24, 25] For this reason, the argument put forward by Kamiura et al. [10] for assigning H2 and H3 to different defects still seems justified. An additional argument is found in the annealing behaviour of these levels.

Figure 6 shows the DLTS spectrum of p-type Ge after a 60 min. anneal at 300 °C, measured in the region between 4 and 5 μm from the junction. For the H3 and H4 peaks a concentration of $4 \pm 1 \times 10^{12} cm^{-3}$ and $4 \pm 1 \times 10^{13} cm^{-3}$ respectively is measured, while there is no indication of the H2 peak. DLTS measurements closer to the surface, show no significant traces of H3. Due to the high leakage current, no additional measurements deeper into the material could be performed.

### B. n-type

It has been reported before that quenching n-type Ge from high temperatures often results in p-type samples, due to the acceptor behaviour of (some of) the induced defects [6, 12]. Our experiments confirm that for higher quenched-in defect concentrations (high $T_H$ or longer $t_Q$), the DLTS-spectrum resembles that of quenched p-type Ge. However, for relatively low $T_H$ and short $t_Q$ it is possible to obtain a sample where the region close to the surface has become p-type, while the interior of the material has remained n-type. The pnp-structure of such sample was verified by DLTS measurements without an additional Au Schottky barrier and by CV measurements. In these structures it is possible to observe both electron (n-region) and hole (p-region) majority carrier traps, as illustrated in figure 7. The spectrum of quenched n-type (650 °C, $t_Q$=5 min.) and p-type (650 °C, $t_Q$= 60 min.) are shown. The trapping parameters of peak E1 are also given in Table I (160K). The resemblance between the peak at 130K of the n-type sample and the H4 peak of

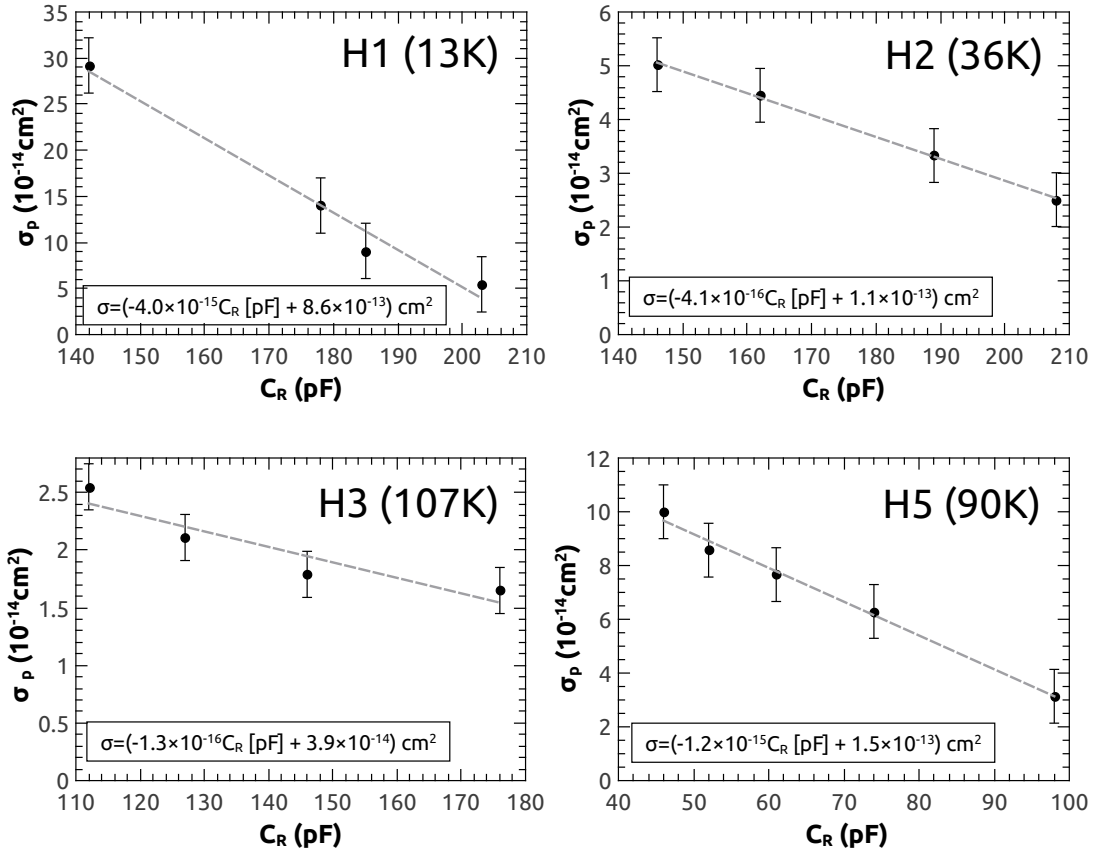


FIG. 4: Reverse capacitance dependence of the (measured) capture cross section of the defect levels. The $C_R$ dependence of the H4 level is plotted in Fig. 3(d).

the p-type sample is striking: most likely this is the H4 peak, measured in the p-region of the sample.

## IV. DISCUSSION

The spectra of quenched p-type Ge agree very well with those reported by Kamiura et al.[10] and exhibit also fair agreement with the spectra in Vanhellemont et al.[6] Kamiura et al. interpreted all observed defect levels as being Cu-related : H1 and H4 were assigned to the 0/- and -/2- levels of substitutional Cu ($Cu_s$), H3 to a donor level of interstitial Cu ($Cu_i^{+/0}$) and H2 to an acceptor level of the $Cu_s$-$Cu_i$ pair. Very probably due to its low concentration, H5 was not noticed, nor discussed. Vanhellemont et al. on the contrary reported that no known Cu-related levels were detected in quenched p-type Ge with DLTS (although $Cu_s$ was clearly detected in far IR absorption measurements), and suggest that all peaks are vacancy-related although most probably not due to the isolated vacancy, which is unstable at RT.

Apparently, in spite of the high resolution of DLTS, identification of defect levels based on their ($\Delta E_A$, $K_T$) signature alone may not always be straightforward. For attractive centers the electric field dependence of the apparent activation energy should be taken into account (PF shift) in comparison with published data. For this reason, including the independently measured capture cross section (via pulse width variation experiments) in the comparison may be very helpful, and we will do this here wherever possible. In Table II our spectroscopic results for levels H1, H4 and E1 are compared with literature data for the three $Cu_s$ levels in Ge, intentionally doped with Cu [40, 41]. The resemblance is striking, especially for the capture cross sections and for the activation energies after PF correction. Obviously, the agreement in capture cross section could only be obtained after the elaborate analysis, presented in Section III A 2, properly taking into account the effects of slow capture.

The assignment of these three levels to Cu may thus be regarded as very reliable. The fact that we observe considerable signals for Cu even in the quenched n-type samples (both in the n- and in the p-type region after heating for only very short time), make it very unlikely that samples studied by Vanhellemont et al. would not have suffered from Cu contamination. The close resemblance

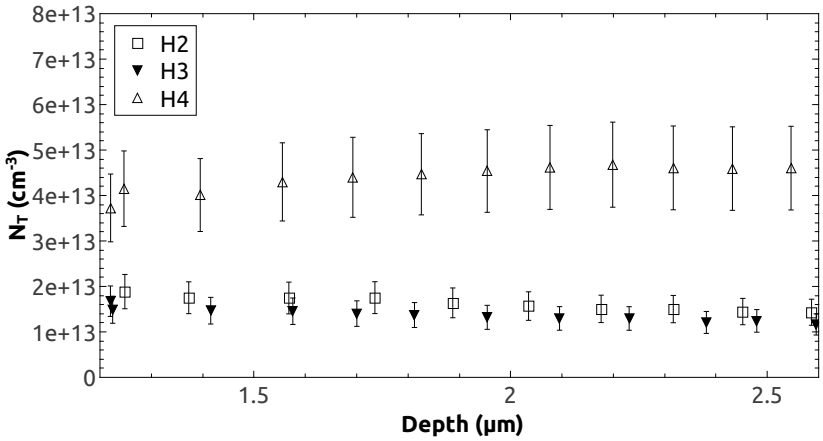


FIG. 5: Depth profile of the different DLTS peaks($t_Q$=60 min., $T_H$=650°C).

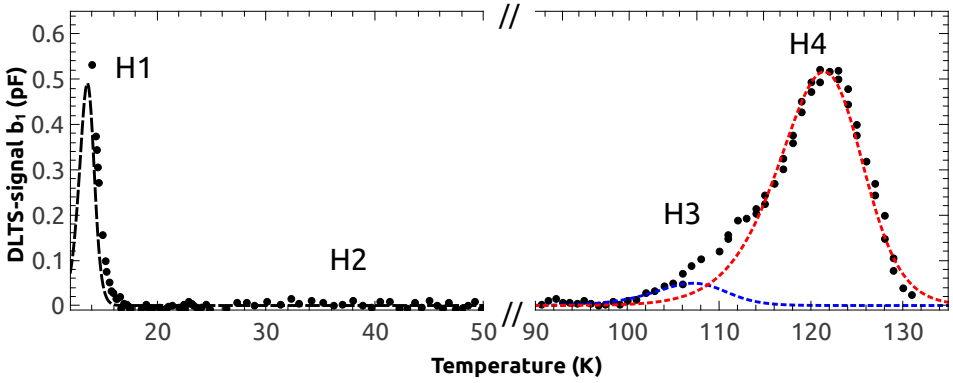


FIG. 6: DLTS spectrum of a p-type Ge sample which was quenched in silicone oil ($t_Q$=60 min., $T_H$=650°C) after a 60 min. post anneal at 300°C. ($V_R$=-5V, $V_P$=-3V). The dashed lines are simulations of the H1, H3 and H4 peak.

| ID | $\Delta E_A$ (meV) | $K_T$ ($s^{-1}K^{-2}$) | $\sigma_p$ ($cm^2$) |
|---|---|---|---|
| H1 | 44 | $2.0 \times 10^7$ | $8.6\times 10^{-13}$ (13K) |
| $Cu_s^{0/-}$ [40] | 37 | $6.0 \times 10^7$ | $2.4 \times 10^{-12}$ (22K) |
| H4 | 328 | $3.9 \times 10^8$ | $9.9\times 10^{-14}$ (123K) |
| $Cu_s^{-/2-}$ [40] | 322 | $1.5 \times 10^9$ | $2.0\times 10^{-13}$ (145K) |
| ID | $\Delta E_A$ (meV) | $K_T$ ($s^{-1}K^{-2}$) | $\sigma_n$ ($cm^2$) |
| E1 | 356 | $4.3 \times 10^7$ | $4.8\times 10^{-19}$ (160K) |
| $Cu_s^{2-/3-}$ [41] | 324 | $3.7 \times 10^6$ | $3.0\times 10^{-19}$ (160K) |

TABLE II: Comparison between $\Delta E_A$, corrected for PF shift and majority capture cross section $\sigma$ reported in literature and calculated in present work.

between spectra also suggests that the most prominent DLTS peaks in the spectra reported by Vanhellemont et al. are most probably due to $Cu_s$. In addition to slow capture (for determining $\sigma_p$) and electric field shifts, the smaller rate window times used in the study of Vanhellemont et al., leading to completely overlapping H3 and H4 peaks, may also have contributed to inaccurate peak assignments. It is worth noting that the Cu concentration measured in our DLTS experiments corresponds only to about 4% of the solubility limit at $T_H$=650°C. [7, 22] It is well-documented that heat treatments of Ge often lead to Cu contaminations [6, 11, 14, 16]. The specific source of this contamination is, however, not clear and could, in particular, not be determined via additional analytical chemistry measurements.

The assignment of H2 and H3 is far less straightforward. In Section III A 3 we established that, in spite of their very similar concentration profiles, these peaks belong to distinct defects. As already mentioned, Kamiura et al. assigned these to an acceptor level of the ($Cu_s$-$Cu_i$) complex and a donor level of $Cu_i$. In this scheme, the post-quench annealing results were explained by the

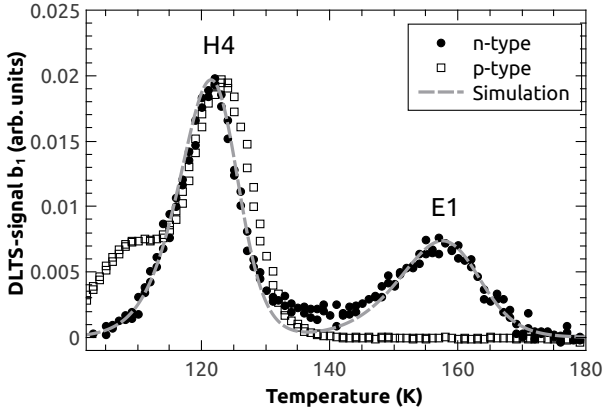


FIG. 7: DLTS spectrum of both quenched n-type ($T_H$=650°C, $t_Q$=5 min.) and p-type (650°C, $t_Q$=60 min.). $V_R$=-1V, $V_P$=-0.2V and $t_W$=512 ms, $t_P$=200 ms for both samples.

following reactions :

$$\begin{cases} H2 \rightleftharpoons Cu_s + H3 \\ H3 \rightarrow sinks \end{cases} \quad (5)$$

hence identifying the H3 defect as interstitial $Cu_i$ and the H2 defect as the $Cu_i$-$Cu_s$ pair. Our experimental results are not in contradiction with this proposal, but it is still worth comparing the DLTS results for quenched-in defects with the recent literature on radiation defects in Ge.[27–35] No metal related carrier traps are expected to be produced in Ge by irradiation at RT or lower temperatures. In spite of the largely different energies involved in the two defect creation processes, it may still be expected that relatively simple intrinsic point defects are created in both. Obviously, only centers that have been reported, or at least suggested, to be stable at RT need to be included in the discussion. It is also worth mentioning that the annealing results of Kamiura et al., which point to a slight increase of the H1 and H4 concentrations after post-quench anneal, suggest that at least either H2 or H3 is Cu-related.

Figure 8 shows the experimental (symbols) Arrhenius diagram for H2 (a) and H3 (b) along with simulations based on the signatures of radiation-induced centers in Ge whose stability at RT has been experimentally proven or suggested.

The signature of H2 appears to agree fairly well with that of two radiation-induced defect levels in Ge, H70 and H80, especially if one considers that these hole-attracting centers are subject to PF shifting.

Based on the Arrhenius plot of the literature data alone it is difficult to assess the difference between these two defects and, if a clear difference exists, which one of these would correspond better to the H2 defect. However, the apparent cross section of H2 ($\sigma_p$=1.1×10$^{-13}$cm$^2$) is in fair agreement with that of H80 ($\sigma$=6×10$^{-14}$cm$^2$)[35], and not with that of H70 ($\sigma_p$=1.3×10$^{-15}$cm$^2$)[34]. This resemblance in $\sigma$, combined with the similar Arrhenius plot, makes it reasonable to assume that H2 is the H80 level observed by Petersen et al. which was tentatively assigned to $V_3^{0/-}$. Although this assignment still is topic of discussion, it is practically excluded that the defects observed after irradiation would be related to Cu or any other TM impurity. This comparison thus shows that a vacancy cluster model for the H2 defect should be taken into consideration.

For H3 none of the reported radiation-induced centers seem to fit. Hence, it seems plausible to identify H3 as Cu-related center. $Cu_i$, which is expected to behave as a donor and was suggested by Kamiura et al., is indeed a good candidate, in agreement with the absence of PF shift for this center. It should be kept in mind, though, that establishing this (non)shifting is not obvious as H3 always occurs as a shoulder on H4.

Finally, the assignment of the H5 peak is briefly discussed. The capture cross section, apparent activation energy and pre-exponential factor here measured agree very well with these of $Ni_s^{0/-}$ ($E_A$=217 meV, $K_T$ =5.8×10$^8$ s$^{-1}$K$^{-2}$, $\sigma_p$ ∼10$^{-13}$ cm$^2$).[22, 42] Although H5 is detected in most heated and quenched p-Ge samples, its amplitude varies considerably from sample to sample and is typically much smaller than that of the H1 and H4 peaks of $Cu_s$. This appears to be in agreement with the ∼ 10 smaller solubility of Ni in Ge, in comparison with Cu, although for both metals concentrations far below these concentration limits at $T_H$ are measured.[7, 43] The specific origin of this contamination remains, even more than for Cu, unclear.

## V. CONCLUSIONS

In this work, DLTS experiments were performed on n- and p-type Ge samples, quenched in a setup based on IR-lamp heating. It was shown that capture in the transition region has a prominent influence on all measured defect levels. To obtain reliable capture cross section parameters -excluding the effect of slow capture- an empirical analysis approach was presented, measuring the $V_R$ dependence of the apparent capture cross section. The obtained capture and emission parameters were compared with those of defect levels of TM impurities in Ge and with those of intrinsic defect levels, recently reported for irradiated Ge. In n-type Ge, a defect level which could be assigned to $Cu_s^{2-/3-}$ was detected. In p-type Ge, five defect levels were present, two of which were assigned to substitutional Cu (H1: $Cu_s^{0/-}$, H4: $Cu_s^{-/2-}$) and one to $Ni_s^{-/2-}$ (H5). For the H3 level an earlier assignment to $Cu_i$ seems plausible. The fifth defect level (H2), previously assigned to the $Cu_i$-$Cu_s$ complex, also corresponds quite well to a vacancy-related defect observed in the

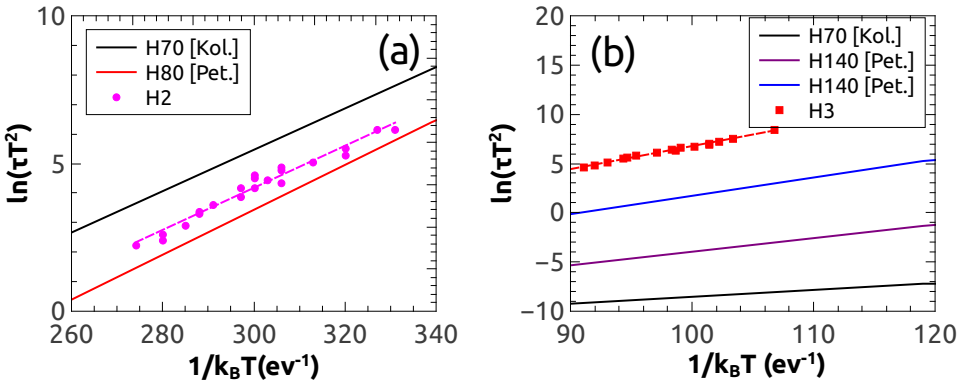


FIG. 8: Arrhenius diagrams of H2 and H3 with linear fits (dashed lines, parameters in table I) and simulations for radiation-induced centers in Ge (full lines). [Pet.] after Petersen et al.[35], [Kol.] after Kolkovsky et al.[34]

DLTS spectra of irradiated Ge.

## ACKNOWLEDGMENTS

The authors thank Umicore for providing the Ge samples investigated in this work, and in particular dr. Kristof Dessein and Dimitri Bluekens for the GDMS analyses. We acknowledge Olivier Janssens and Nico De Roo for the EDX and XPS measurements. The CoCooN research group (prof. C. Detavernier, Ghent University, dept. Solid State Sciences) is thanked for help with the XRF measurements and dr. Bart Vekemans (Ghent University - Dept. Analytical Chemistry) for help with the interpretation. The authors acknowledge the FWO for financial support through grant no G.0207.10N.

## REFERENCES

[1] J. Vanhellemont and E. Simoen, J. Electrochem. Soc. **154**, H572 (2007).
[2] R. A. Logan, Phys. Rev. **101**, 1455 (1956).
[3] B. Samuelsson, Arkiv för Fysic **35**, 321 (1967).
[4] R. N. Hall, Lattice Defects in Semiconductors **23**, 190 (1974).
[5] W. Lerch, N. A. Stolwijk, and H. Mehrer, Meas. Sci. Technol. **5**, 835 (1994).
[6] J. Vanhellemont, J. Lauwaert, A. Witecka, P. Spiewak, I. Romandic, and P. Clauws, Physica B **404**, 4529 (2009).
[7] C. Claeys and E. Simoen, eds., *Germanium-Based Technologies* (Elsevier, 2007).
[8] J. Broeckx, Y. Kamiura, P. Clauws, and J. Vennik, Solid State Commun. **40**, 149 (1981).
[9] J. Broeckx, Y. Kamiura, P. Clauws, and J. Vennik, Solid State Commun. **38**, 883 (1981).
[10] Y. Kamiura and F. Hashimoto, Jpn. J. Appl. Phys **28**, 763 (1989).
[11] S. Mayburg, Phys. Rev. **95**, 38 (1954).
[12] S. Mayburg, Phys. Rev. **103**, 1130 (1956).
[13] A.Hiraki, J. Phys. Soc. Jpn **21**, 34 (1966).
[14] A. Tweet, J. Appl. Phys. **30**, 2002 (1959).
[15] Y. Kamiura, F. Hashimoto, H. Sugiyama, and S. Yoneyama, Jpn. J. Appl. Phys **21**, L357 (1982).
[16] T. Hattori, T. Takada, K. Kagawa, A. Mitsuishi, and Y. Kamiura, Phys. Stat. Sol. a **120**, K63 (1990).
[17] N. Stolwijk, W. Frank, J. Holzl, S. Pearton, and E. Haller, J. Appl. Phys. **57**, 5211 (1985).
[18] H. Bracht, N. Stolwijk, and H. Mehrer, Phys. Rev. B **43**, 14465 (1991).
[19] H. Bracht, Mat. Sci. Semicon. Proc. **7**, 113 (2004).
[20] D. V. Lang, J. Appl. Phys. **45**, 3023 (1974).
[21] S. Forment, J. Vanhellemont, P. Clauws, J. Van Steenbergen, S. Sioncke, M. Meuris, E. Simoen, and A. Theuwis, Mat. Sci. Semicon. Proc. **9**, 559 (2006).
[22] P. Clauws and E. Simoen, Mat. Sci. Semicon. Proc. **9**, 546 (2006).
[23] P. Clauws, J. Van Gheluwe, J. Lauwaert, E. Simoen, J. Vanhellemont, M. Meuris, and A. Theuwis, Physica B **401-402**, 188 (2007).
[24] J. Lauwaert, J. Van Gheluwe, J. Vanhellemont, E. Simoen, and P. Clauws, J. Appl. Phys. **105**, 073707 (2009).
[25] J. Lauwaert, J. Vanhellemont, E. Simoen, H. Vrielinck, and P. Clauws, J. Appl. Phys. **111**, 113713 (2012).
[26] F. Poulin and J. C. Bourgoin, Phys. Rev. B **26**, 6788 (1982).
[27] V. Emtsev, Materials Science in Semiconductor Processing **9**, 580 (2006).
[28] C. Lindberg, K. Nielsen, A. Mesli, and A. N. Larsen, Mater. Sci. Semicond. Process. **9**, 597 (2006).
[29] V. P. Markevich, Mat. Sci. Semicon. Proc. **9**, 589 (2006).
[30] V. Kolkovsky, M. Petersen, and A. Larsen, Appl. Phys. Lett. **90**, 112110 (2007).
[31] V. Kolkovsky, M. Petersen, A. Mesli, J. V. Gheluwe, P. Clauws, and A. Larsen, Phys. Rev. B **78**, 233201 (2008).
[32] V. Kolkovsky, M. Petersen, A. Larsen, and A. Mesli,

Mater. Sci. Semicond. Process. **11**, 336 (2008).
[33] A. Mesli, L. Dobaczewski, K. B. Nielsen, V. Kolkovsky, M. Petersen, and A. N. Larsen, Phys. Rev. B **78**, 165202 (2008).
[34] V. Kolkovsky, M.C.Petersen, A. Mesli, and A. Larsen, Phys. Rev. B **81**, 035208 (2010).
[35] M. Petersen and A. Larsen, Phys. Rev. B **82**, 075203 (2010).
[36] A. Witecka, Master's thesis, Warsaw University of Technology (2009).
[37] D. Pons, J. Appl. Phys. **55**, 33644 (1984).
[38] J. Lauwaert, J. Van Gheluwe, and P. Clauws, Rev. Sci. Instr. **79**, 093902 (2008).
[39] S. H. Segers, J. Lauwaert, P. Clauws, E. Simoen, J. Vanhellemont, F. Callens, and H. Vrielinck, J. Phys. D: Appl. Phys. **404**, 4529 (2013).
[40] E. Simoen, P. Clauws, M. Lamon, and J. Vennik, Semicond. Sci. Technol. **1**, 53 (1986).
[41] P. Clauws, G. Huylebroeck, E. Simoen, P. Vermaercke, F. De Smet, and J. Vennik, Semicond. Sci. Technol. **4**, 910 (1989).
[42] G. Huylebroeck, P. Clauws, E. Simoen, and J. Vennik, Solid State Commun. **82**, 367 (1992).
[43] P. Penning, Phys. Rev **102**, 1414 (1956).